Silicene Nanoribbons on an Insulating Thin Film

Khalid Quertite, Hanna Enriquez, Nicolas Trcera, Yongfeng Tong, Azzedine Bendounan, Andrew Mayne, Gérald Dujardin, Pierre Lagarde, Abdallah El Kenz, Abdelilah Benyoussef, et al.

COMPELING EVIDENCE OF SILICENE SYNTHESIS ON AN INSULATING THIN FILM

Khalid Quertite[1,2,3], Hanna Enriquez[1], Nicolas Trcera[2], Yongfeng Tong[2], Azzedine Bendounan[2], Andrew J. Mayne[1], Gérald Dujardin[1], Pierre Lagarde[2], Abdallah El kenz[3], Abdelilah Benyoussef[3,4], Yannick J. Dappe[5], Abdelkader Kara[6], and Hamid Oughaddou[1,7]

[1]Université Paris-Saclay, CNRS, Institut des Sciences Moléculaires d'Orsay (ISMO), Bât. 520, 91405 Orsay, France

[2]Synchrotron Soleil, L'Orme des Merisiers, Saint-Aubin, B.P. 48, 91192 Gif-sur-Yvette Cedex, France

[3]LaMCScI, Faculté des Sciences, Université Mohammed V - Agdal, 10100, Rabat, Morocco

[4]Hassan II Academy of Sciences and Technology, Rabat, Morocco

[5]Université Paris-Saclay, CEA, CNRS, SPEC, 91191 Gif-sur-Yvette Cedex, France

[6]Department of Physics, University of Central Florida, Orlando, FL 32816, USA

[7]Département de Physique, CY, Cergy Paris Université, 95031 Cergy-Pontoise Cedex, France

Abstract

The discovery of graphene[1,2], with its unique physical properties has driven an intense research effort to find new 2D materials based on other elements[3,4]. Many have been discovered: boron nitride[5], silicene[6-12], germanene[7,13-14], phosphorene[15,16], stanene[17], and metal dichalcogenides[18-19]. The widespread use of silicon in modern technology makes silicene a particularly logical choice. A silicene-based field effect transistor operating at room temperature has been demonstrated recently[20]. However, producing free-standing silicene has proved to be a huge challenge. Until now, silicene could be synthesized only on metal surfaces where it naturally forms strong interactions with the metal substrate that modify its electronic properties. Here, we report the first experimental evidence of silicene sheet on an insulating NaCl thin film. This work represents a major breakthrough; for the study of the intrinsic properties of silicene, and by extension to other 2D materials that have so far only been grown on metal surfaces.

Among the properties unique to 2D materials, silicene should show a quantum spin Hall effect[21], and giant magnetoresistance[22]. For historical reasons[9-10], the early investigations of silicene were performed almost exclusively on metal substrates by epitaxial growth of silicon atoms: Si/Ag[8-10], Si/Au[11-12], Si/ZrB_2[23], and Si/Ir[24]. However, a number of questions remained unanswered due to diverging evidence, crucially over the existence or not of Dirac fermions in silicene. Angular-resolved photoemission spectroscopy (ARPES) and scanning tunneling spectroscopy (STS)[25,26] claimed to observe them, while other experiments indicated a strong interaction between silicene and the metallic surfaces[27,28], indicating that the observed linear dependence was due to an interface state of the silver. Using a metal substrate was obviously a hindrance to observing the intrinsic properties of silicene. This alone has motivated the exploration of other potential substrates to reduce the interaction with silicene. From this point of view, Alkali metal halides, such as NaCl, present an ideal alternative substrate, particularly in the form of a thin film, simply because the thin NaCl film behaves as a dielectric layer which decouples the electronic states of adsorbed species[29-31] from the metallic substrates.

Here, we present a comprehensive study of the growth of silicene on a thin NaCl film deposited on the Ag(110) surface. Using scanning tunneling microscopy (STM), low energy electron diffraction (LEED), X-ray photoemission spectroscopy (XPS), extended x-ray absorption fine structure spectroscopy (EXAFS) and density functional theory (DFT) calculations, we demonstrate that silicene forms an extended 2D structure on the thin NaCl film. The STM images show a highly ordered sheet with honeycomb-like structure. The XPS and EXAFS measurements reveal that the silicon atoms have a single chemical environment, and that the silicon environment is consistent with that of silicene. Finally, DFT calculations confirm the formation of weakly bound silicene

composed of a densely packed array of nanoribbons on the NaCl film in line with the experimental results. This is the first clear evidence of the formation of silicene on an insulating thin film. The best growth conditions for obtaining large-area NaCl thin films on the Ag(110) surface has already been optimized successfully[32] (see Methods).

Figure 1 presents the LEED patterns obtained on a) the bare Ag(110) surface, b) after deposition of ~ 1 ML of NaCl, and c) after the deposition of about 1 ML of silicon on the NaCl/Ag(110) surface, respectively. Figure 1-a shows a sharp (1x1) pattern characteristic of the clean Ag(110) surface. In Figure 1-b, the formation of the NaCl layer creates a (4x1) superstructure with respect to the Ag unit cell. In Figure 1c, the LEED pattern presents a (3x4) superstructure of the Silicene layer with respect to the Ag unit cell. In both Figures 1-b and 1-c, the underlying layers of Ag and NaCl/Ag, respectively, are visible through the top layer.

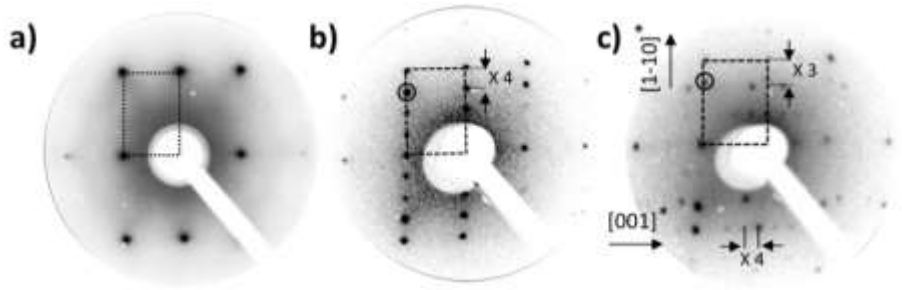

Figure 1: LEED patterns of (a) bare Ag(110) substrate, (b) after a deposition of ~ 1 ML of NaCl, (c) after the deposition of ~ 1 ML of silicon on NaCl/Ag(110). The Ag(110) unit cell, the x3 and x4 periodicities are indicated. The diffraction spot corresponding to NaCl film is highlighted by the small black circles in b and c. The LEED patterns were recorded at an energy of 70 eV.

Figure 2a shows a typical STM image of the thin NaCl film grown on Ag(110). It is well known that NaCl forms islands on different metallic substrates[33-36]. In this experiment, the surface is covered by NaCl islands more than 160 x 160 nm^2 in size, with very few bare areas of silver still remaining. The equivalent of 1 ML of silicon was then deposited on the NaCl/Ag(110) surface. The STM

topography in Figure 2b shows a Si layer that covers the entire surface of the NaCl film. Figure 2c displays a close-up of the STM image (Figure 2b). The image shows hexagons of Si atoms forming a chain-like structure all oriented along the same [1-10] direction. Figure 2d displays an atomically resolved image of these chains revealing a highly ordered honeycomb-like structure. The line profiles recorded along the lines A and B in Figure 2d are shown on Figure 2e and 2f respectively. In these line profiles we observe a periodicity of 0.86 nm and 1.60 nm, respectively, in good agreement with the (3x4) LEED pattern. Indeed, 0.86 nm corresponds to 3x $a_{Ag[1-10]}$ and 1.60 nm corresponds to 4x$a_{Ag[001]}$ ($a_{Ag[1-10]}$ = 0.289 nm and $a_{Ag[001]}$ = 4.07 nm). In addition, the line profile C along the edge of the hexagon in Figure 2d, gives a lateral distance between the two nearest protrusions of 0.45 nm with a very small buckling (see figure 2g). The distance between the nearest-neighbor protrusions is larger than the Si-Si distance of 0.23 nm measured in other hexagonal silicene layers indicating that only some of the atoms contribute to the Density of States (DOS) in these STM images.

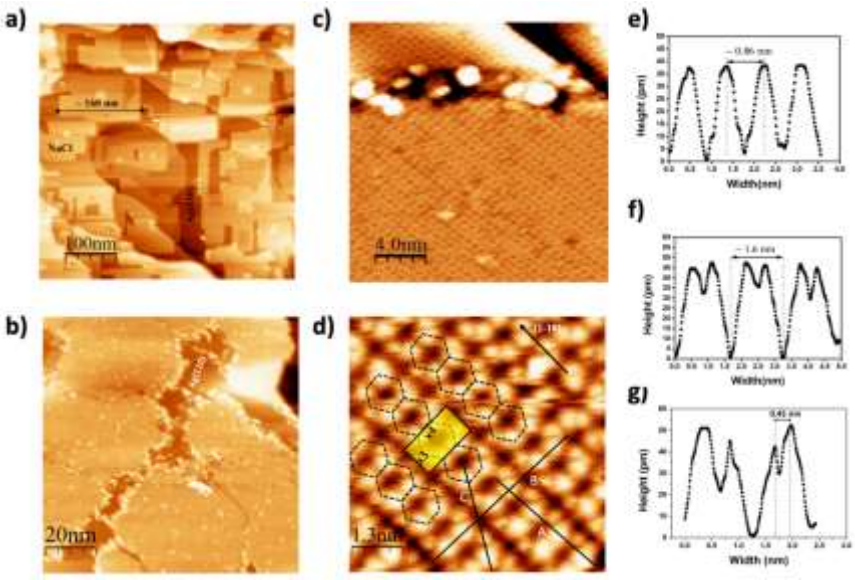

Figure 2: Occupied-state STM images corresponding to (a) 1ML NaCl film on Ag(110) (500x500 nm^2, U= -1.05 V, I= 0.7 nA), (b) 1 ML of silicon deposited over the NaCl film (100x100 nm^2, U= -1V,

I= 0,8 nA), (c) zooming on Figure 2b (20x20 nm², U= -0.7 V, I= 0.8 nA), (d) High-resolution STM image on silicon layer (6.5x6.5 nm², U= -0.04 V,I= 2.6 nA). (e), (f) and (g) are line scans corresponding to A, B and C on Figure 2d respectively.

The electronic structure of the silicene layer can be understood further using X-ray photoemission spectroscopy to probe the environment of the Si atoms within the silicene layer. The peaks corresponding to the Ag 3d, Si 2p, Cl 2p and Na 2s core levels were fitted with spin-orbit split Doniach-Sunjich (D-S) function[37] (see Methods). First, the Ag 3d core level spectra recorded at normal emission (0° to the surface normal), with a photon energy of 700 eV, before and after deposition of the NaCl film are shown in Figure 3a and 3b, respectively.

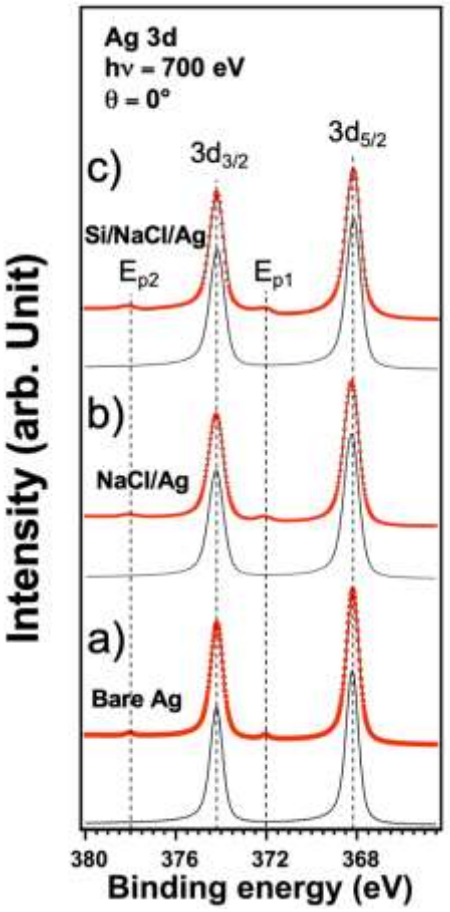

Figure 3: High-resolution core level spectra of Ag 3d recorded on bare Ag(110) surface (a) and after deposition of NaCl film (b) and after deposition on Silicon layer on NaCl (c). Dots correspond

to data and black line overlapping the data corresponds to the best fit. For each spectrum, the component giving the best fit is indicated in black.

On the bare Ag(110) substrate, we observe two peaks in the XPS spectra at binding energies of 374.2 eV and 368.2 eV corresponding to the Ag $3d_{3/2}$ and $3d_{5/2}$ core level peaks. The peaks require a fit with only one spin–orbit split component, and are located energies similar to those reported in the literature[38]. The two small peaks located at E_{P1} = 372.0 eV and E_{P2} = 378.0 eV are the two dominant plasmon excitations of silver[37]. After deposition of the NaCl film on Ag(110), the Ag 3d peaks are located at the same binding energies, and only one spin–orbit split component is required to fit the Ag 3d core level. This indicates that the interaction between Ag and NaCl is weak as expected. The two plasmon peaks of silver are still visible after deposition of NaCl indicating that the NaCl film has not affected the surface plasmons at the NaCl/Ag interface.

Figure 3c shows the Ag 3d after deposition of the silicon layer on NaCl/Ag(110). Here again only one spin–orbit split component is required to fit the Ag 3d core level. We observe that the deposition of silicon does not affect the plasmon peaks of silver. That they are still visible is an indication that Si atoms have not adsorbed on Ag surface, since these plasmons would be quenched following the adsorption of silicon on Ag(110) as has been shown previously[39]. It is clear that the silicene layer has grown on top of the NaCl layer.

To complete the observations, the Cl 2p and Na 2s core level spectra were recorded, in normal emission (0°) at photon energies of 700 eV and 147 eV, respectively, after deposition of Si deposition on NaCl/Ag(110). In Figure 4a and 4b, the Cl and Na spectra require only one spin–orbit split component to fit the spectra. This indicates that Na and Cl ions have only one chemical environment (Na surrounded by Cl atoms and Cl atoms surrounded by Na). This again is further

evidence for a weak interaction both between the NaCl film and Si as well between the NaCl film and the silver substrate. Finally, Figure 4c presents the Si 2p core level spectra of the silicon layer recorded in normal emission (0°) at a photon energy of 147 eV. The Si 2p spectrum requires only one spin-orbit split component to fit the spectrum indicating that the silicon atoms are all equivalent in having only one chemical environment. Given that Si atoms are adsorbed on top of the NaCl film, this indicates that the Si-NaCl interaction is weak. This contrasts clearly with previous XPS studies of silicon on silver surfaces that showed two distinct components resulting from the two Si-Si and Si-Ag environments[9-10,40].

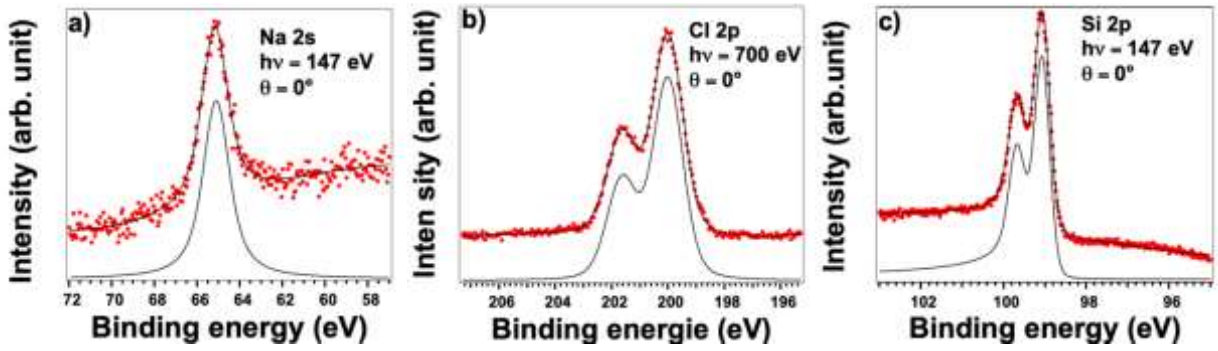

Figure 4: High-resolution core level spectra corresponding to: (a) Na 2s, (b) Cl 2p, recorded after deposition of 1 ML of NaCl on Ag(110), (c) Si 2p, recorded after deposition of 1 ML over NaCl/Ag(110). All spectra are recorded at normal emission (0°). Dots correspond to the raw data and the overlapping black line corresponds to the best fit. For each spectrum, the component giving the best fit is indicated in black.

EXAFS measurements recorded at the Si K-edge provide complementary information on the local structure of the 2D silicon layer grown on NaCl/Ag(110) surface. EXAFS spectra give a precise determination of the interatomic distance between the excited atom (here Si) and its neighbors. Figure 5 shows the modulus and the imaginary part of the Fourier transform of $k^3X(k)$ for bulk silicon and for the silicon layer grown on NaCl/Ag(110) surface. First, there is a high similarity between the two local structures. This indicates that the local structure around the Si atoms of

the silicon layer is highly ordered. The peaks located at 1.92 Å and 3.4 Å in Figure 5a are assigned to the first and second interatomic distances in the bulk silicon crystal[41]. These values are shifted with respect to the expected lattice parameters of 2.35 Å and 3.83 Å due to the well-known effect of the phase shift between the absorbing atom and the backscattering one[42]. The first and second interatomic Si-Si distances from the EXAFS spectra are very close to the values reported for silicene grown directly on Ag(110) or Ag(111) surfaces[41]. However, an interatomic distance of 2.7 Å was attributed to the Si-Ag bond[41]. In our study, this particular distance is not observed so Si-Ag bond formation is absent. Again, this indicates that the Si atoms are located on top of NaCl film. Taking together all the information from the STM, XPS and EXAFS studies, we can conclude that silicon atoms form a 2D layer with a local structure similar to silicene decoupled from silver substrate by the thin NaCl film.

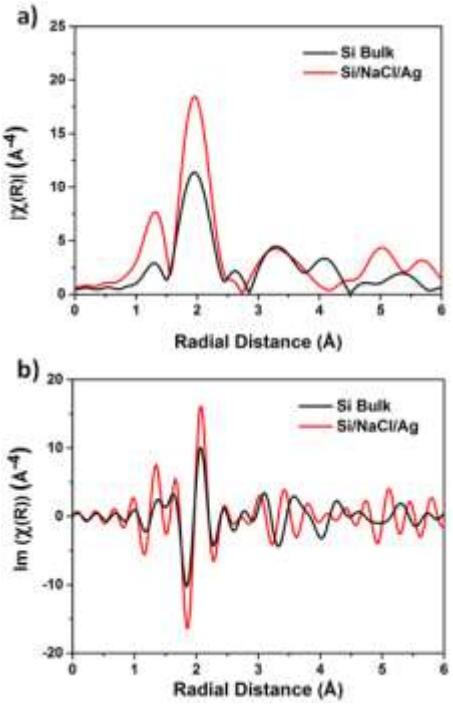

Figure 5: (a) modulus and (b) imaginary parts of the Fourier transforms of bulk silicon and 2D Si sheet deposited on NaCl/Ag(110)

To support the experimental findings, a computational study was performed using Density Functional Theory (DFT) (see Methods). From the LEED pattern shown in Figure 1b, along the close-packed direction, 3 Na-Na (or Cl-Cl) distances correspond to 4 Ag-Ag distances. Since the periodicity along this direction was x3 in the LEED after deposition of silicon (see Figure 1c), we have chosen a slab of 12 Ag-Ag lengths along this direction. As the NaCl and silicene layers form x1 and x4 periodicities along the direction perpendicular to the channels respectively (see Figure 1b and 1c), a x4 was adopted along this direction. The corresponding silicene structure which fulfills all these conditions is a silicene nanoribbon aligned along the long direction of the 12 by 4 slab. Obviously, the resulting dangling bonds at the edge of the ribbon will have a strong influence on the electronic structure, and to overcome this difficulty, we have added hydrogen atoms in order to saturate these bonds. This is fully justified by the presence of residual hydrogen in the vacuum chamber which is known to react with semiconductor surfaces even at very low pressure (10^{-11} mbar)[43]. We have optimized this hydrogen-terminated structure using the DFT calculations. Figure 6 shows the top and side views of the relaxed system. After full relaxation of the system, we found an interlayer distance of 0.33 nm between the silicene sheet and the NaCl layer. The silicene sheet is much more corrugated than in the gas phase with a maximum corrugation of 0.67 Å. Note that even after having chosen a 12x4 cell of silver for the calculation, the Si presents a (3x4) structure with respect to the silver in good agreement with STM and LEED results. The (1x1) and the (3x4) cells are indicated in Figure 6. The first nearest neighbor Si-Si average distance is found to be 0.237 nm in good agreement with the EXAFS results and with the values reported previously for Silicene/Ag[41]. The separation between silicene layer and the NaCl of 0.33 nm is similar to that found in graphite. Taking into consideration the adsorption energy values of around

50 meV/atom as well, is strong evidence that silicene is held on the substrate by weak electrostatic van der Waals forces.

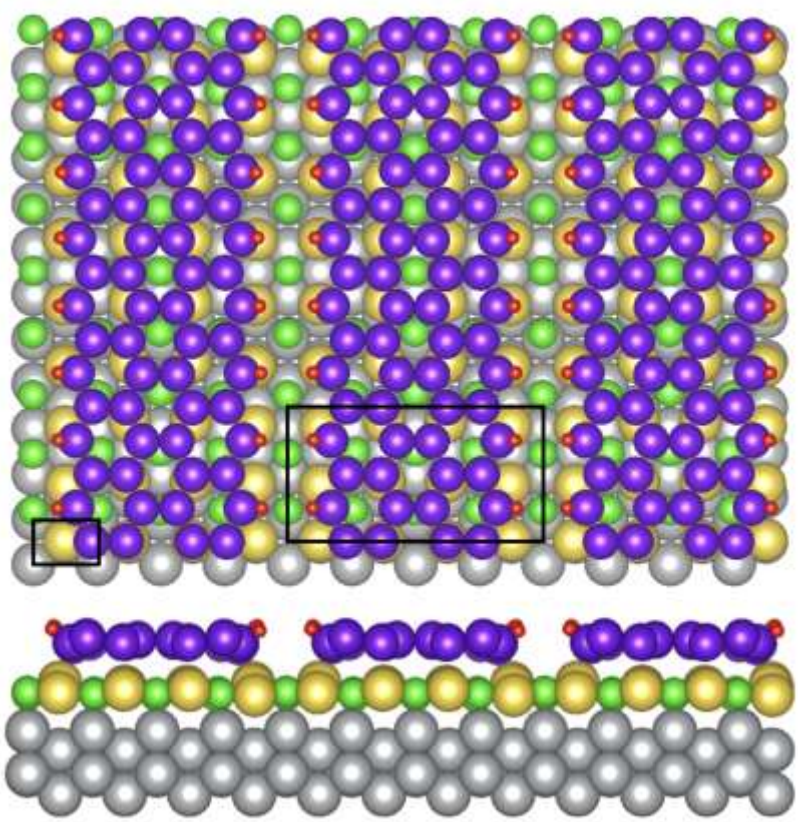

Figure 6: Top view (up) and side view (down) of silicene nanoribbons on Ag(110), after full relaxation. Ag, Cl, Na, H, and Si atoms are in grey, green, yellow, red and blue purple. Top view (up) and side view (down). The (1x1) and the (3x4) cells are indicated by the small and large rectangles, respectively.

Methods

The experiments were performed in ultra-high vacuum apparatus with pressure in the 10^{-11} mbar range, equipped with special tools for surface preparation and characterization: an ion gun for surface sputtering, Low Energy Electron Diffraction (LEED), Auger electron spectroscopy (AES) and a commercial Omicron LT-STM. The growth of NaCl and Silicon was controlled systematically by Auger and LEED measurements.

Surface preparation

The Ag(110) commercial crystal with 99.99999% purity was cleaned by multiple cycles of sputtering (650 eV Ar^+ ions, P ~ 10^{-5} mbar) followed by annealing at 500 °C. NaCl deposition was done using a Knudsen cell heated at 520 °C. The Ag substrate was kept at 140°C during NaCl deposition to grow large NaCl islands[32]. Silicon was evaporated (~ 0.02 Si ML/min) by direct current heating of a Si wafer to about 1200 °C onto NaCl/Ag(110) held at 140 °C. A post-annealing was performed at 200 °C in order to improve the diffusion of silicon. All the STM images where recorded at 78 K and Nanotec WSxM software[44] was used to process and analyze the data.

Spectroscopy

The XPS and EXAFS experiments were carried out at TEMPO and LUCIA beam-lines respectively at SOLEIL Synchrotron facility in France. The same Ag(110) crystal was used for all the experiments. The core level spectra were adjusted with spin-orbit split Doniach-Sunjich (D-S) function[40]. The Ag3d was fitted with a 140 meV eV Gaussian profile and a 280 meV Lorentzian profile, the spin-orbit splitting is 6 eV, and the branching ratio is 0.78. The best fit for Cl 2p was obtained with a 0.83 eV Gaussian profile and a 0.12 eV Lorentzian profile, the spin-orbit splitting is 1.63 eV, and the branching ratio is 0.49. For Na 2s, the best fit is obtained with 0.53 eV Gaussian profile and a 0.55 eV Lorentzian profile, while for the Si 2p spectra, the best fit was obtained with a 0.255 eV Gaussian profile, a 0.07 eV Lorentzian profile, the spin-orbit splitting is 0.61 eV, and the branching ratio is 0.48. The background of each spectrum was fitted with polynomic of second order. The EXAFS spectra were collected in total electron yield mode. The full analysis of the experimental data has been conducted with the Athena code[45]. A frequency cutoff below 1.4 Å was used to

filter out the background oscillations and a Kaiser-Bessel window function[46] from k=2 to 9.5 $Å^{-1}$ has been performed before the Fourier transform.

Structure computation

The computational study has been performed using Density Functional Theory (DFT) as implemented in the Fireball code[47]. This code uses the local density approximation (LDA) for the exchange and correlation functional according to the McWeda approach[48] and a combination of atomic-like orbitals as basis set[49]. Basis sets of sp^3d^5 for Ag and Cl, sp^3 for C and Si and s for H and Na were used with cutoff radii (in atomic units) s = 4.5, p = 5.5, d = 4.0 (Ag), s = 3.9, p = 4.4, d = 5.4 (Cl), s = 4.5, p = 4.5 (C), s = 4.8, p = 5.4 (Si), s = 4.1 (H) and s = 8.0 (Na). These basis sets have been already used successfully in the study of graphene and two-dimensional materials[50,51]. We have considered a Ag(110) slab of 5 layers containing 12 atoms each in a 3x4 structure, with a NaCl monolayer on top plus a hydrogenated silicene nanoribbon. Calculations have been performed using a set of 32 k-points in the first Brillouin zone, and structures have been optimized until the forces were lower than 0.1 eV/Å.

Author Contributions:

H.O. conceived and conducted the research project. K.Q., H.E., N.T., Y.T., Az.B., P.L., A.J.M., and H.O. performed the experiments. Y.D. and A. K. performed the calculations. K.Q., H.E., N.T., Y.T., Az.B., P.L., A.E., Ab.B, Y.D., A.K., A.J.M, G.D. and H.O analyzed the results and contributed to the scientific discussions. All the authors contributed to the manuscript preparation.

Competing financial interests:

The authors declare no competing financial interests.

Acknowledgements

This work is supported by a public grant overseen by the French National Research Agency (ANR) as part of the "Investissements d'Avenir" program (Labex NanoSaclay, reference: ANR-10-LABX-0035).

References:

1. Novoselov, K. S. et al. Two-dimensional gas of Dirac fermions in graphene. *Nature* **438**, 197-200 (2005).
2. Geim, A. K. and Novoselov, K. S. The rise of graphene. *Nature Materials* **6**, 183-186 (2007)
3. Mas-Ballesté, R. C. A., Gómez-Navarro, C., Gómez-Herrero, J. and Zamora, F. 2D materials: to graphene and beyond. *Nanoscale* **3**, 20–30 (2011).
4. Gupta, A., Sakthivel, T., & Seal, S. Recent development in 2D materials beyond graphene. *Prog. Mater. Sci.* **73**, 44-126 (2015).
5. Wu, X, Dai, J, Zhao, Y, et al. Two-Dimensional Boron Monolayer Sheets. *ACS Nano* **6**, 7443 (2012).
6. Nature Research highlights. Silicene: Flatter silicon. *Nature Nanotechnology* **5**, 384 (2010).
7. Cahangirov, S., Topsakal, M., Akturk, E., et al. Two- and One-Dimensional Honeycomb Structures of Silicon and Germanium. *Phys. Rev. Lett.* **102**, 236804 (2009).
8. Lalmi, B, Oughaddou, H, Enriquez, H, Kara, A, Vizzini, S. Ealet, B, Aufray, B. Epitaxial growth of a silicene sheet. *Appl. Phys. Lett*. **97**, 223109 (2010).
9. Kara, A, Enriquez, H, Seitsonen, A.P, Voon, L.C.L.Y, Vizzini, S, Aufray, B, Oughaddou, H. A Review on Silicene – new candidate for electronics. *Surf. Sci. Rep.* **67**, 1-18 (2012).
10. Oughaddou, H., Enriquez, H., Tchalalaa, M. R., Yildirim, H., Mayne, A. J., Bendounan, A., Dujardin, G., Ait Ali, M., Kara, A. Silicene, a promising new 2D material. *Progress in Surface Science* **90**, 46-81 (2015).
11. Tchalala, M. R., Enriquez, H., Mayne, A.J, Kara, A, Roth, S, Silly, M. G., Bendounan, B., Sirotti, S., Greber, Th, Aufray, B, Dujardin, G, Ait Ali, A, and Oughaddou, H. Formation of one-dimensional self-assembled silicon nanoribbons on Au(110)-(2x1), *Appl. Phys. Lett.,* **102**, 083107 (2013)
12. Sadeddine, S., Enriquez, H., Bendounan, A., Das, P., Vobornik, I., Kara, A., Mayne, A., Sirotti, F., Dujardin, G., and Oughaddou, H. Compelling experimental evidence of a Dirac cone in the electronic structure of a 2D Silicon layer. *Sci. Rep.* **7**, 44400 (2017).
13. Derivaz, M., Dentel, D., Stephan, R., Hanf, M. C., Mehdaoui, A., Sonnet, P., Pirri, C., Continuous germanene layer on Al(111). *Nano Lett.* **15**, 2510 (2015).
14. Zhang, L., Bampoulis, P., Rudenko, A. N., Yao, Q., Van Houselt, A., Poelsema, B., Katsnelson, M. I., Zandvliet, H. J. W. Structural and Electronic Properties of Germanene on MoS2. *Phys. Rev. Lett.* **116**, 256804 (2016).
15. Favron, A., Gaufrès, E., Fossard, F., Phaneuf-L'Heureux, A.L., Tang, N. Y-W., Lévesque, P.L., Loiseau, A., Leonelli, R., Francoeur, S., Martel, R. Photooxidation and quantum confinement effects in exfoliated black phosphorus. *Nature Materials* **14**, 826 (2015).

16. Zhang, W., Enriquez, H., Tong, Y., Bendounan, A., Kara, A., Seitsonen, A. P., Mayne, A., Dujardin, G., and Oughaddou, H., Epitaxial Synthesis of Blue Phosphorene, *Small* **14** 1804066 (2018)
17. Zhu, F.F., Chen, W.J., Xu, Y., Gao, C.L., Guan, D.D., Liu, C.H., Qian, D., Zhang S.C., Jia, J.F., Epitaxial growth of two-dimensional stanene, *Nature Materials* **14**, 1020 (2015).
18. Butler, SZ, Hollen, SM, Cao, LY, et al. Progress, Challenges, and Opportunities in Two-Dimensional Materials Beyond Graphene. *ACS Nano* **7**, 2898 (2013).
19. Xu, MS, Liang, T, Shi, MM, et al. Graphene-Like Two-Dimensional Materials. *Chem. Rev.* **113**, 3766 (2013).
20. Tao, L. et al. Silicene field-effect transistors operating at room temperature. *Nature Nanotechnology* **10**, 227 (2015).
21. Liu, C-C., Feng, W. & Yao, Y. Quantum spin Hall effect in silicene and two-dimensional germanium. *Phys. Rev. Lett.* **107**, 076802 (2011).
22. Xu, C. et al. Giant magnetoresistance in silicene nanoribbons. *Nanoscale* **4**, 3111–3117 (2012).
23. Fleurence, AFR., Ozaki, T., Kawai, H., Wang, Y., Yukiko, YT. ; Experimental evidence for epitaxial silicene on diboride thin films. *Phys. Rev. Lett.* **108**, 245501 (2012).
24. Meng, L, Wang, Y, et al. Buckled Silicene Formation on Ir(111). *Nano Lett.* **13**, 685 (2013)
25. Vogt, P, De Padova, P, Quaresima, C, Avila, J, Frantzeskakis, E, Asensio, M.C, Resta, A, Ealet, B, Le Lay, G. Silicene: compelling experimental evidence for graphenelike two-dimensional silicon. *Phys. Rev. Lett.* **108**, 155501 (2012).
26. Chen, L, Liu, C.C, Feng, B, He, X, Cheng, P, Ding, Z, Meng, S, Yao, Y, Wu, K. Evidence for Dirac Fermions in a Honeycomb Lattice Based on Silicon. *Phys. Rev. Lett.* **109**, 056804 (2012).
27. Lin, C.L, Arafune, R, Kawahara, K, Kanno, M, Tsukahara, N, Minamitani, E, Kim, Y, Kawai, M, Takagi, N. Substrate-Induced Symmetry Breaking in Silicene. *Phys. Rev. Lett.* **110**, 076801 (2013).
28. Wang, Y.P, Cheng, H.P. Absence of a Dirac cone in silicene on Ag(111): First-principles density functional calculations with a modified effective band structure technique. *Phys. Rev. B* **87**, 245430 (2013).
29. Repp, J., Meyer, G., Stojković, S.M., Gourdon, A. and Joachim, C., Molecules on insulating films: scanning-tunneling microscopy imaging of individual molecular orbitals. *Phys. Rev. Lett.* **94**, 026803 (2005).
30. Doppagne, B., Chong, M.C., Lorchat, E., Berciaud, S., Romeo, M., Bulou, H., Boeglin, A., Scheurer, F. and Schull, G., Vibronic Spectroscopy with Submolecular Resolution from STM-Induced Electroluminescence. *Phys. Rev. Lett.* **118**, 127401 (2017).
31. Repp, J., Meyer, G., Olsson, F.E. and Persson, M., Controlling the charge state of individual gold adatoms. *Science* **305**, 493-495 (2004).
32. K. Quertite, K. Lasri, H. Enriquez, A. Mayne, A. Bendounan, G. Dujardin, N. Trcera, W. Malone, A. El Kenz, A. Benyoussef, A Kara, and H. Oughaddou, Atomic Structure of Submonolayer NaCl Grown on Ag(110) Surface, *J. Phys. Chem. C* **121**, 20272-20278 (2017)
33. Repp, J., Meyer, G. and Rieder, K.H., Snell's law for surface electrons: Refraction of an electron gas imaged in real space. *Phys. Rev. Lett.* **92**, 36803 (2004).

34. Repp, J., Meyer, G., Paavilainen, S., Olsson, F.E. and Persson, M., Scanning tunneling spectroscopy of Cl vacancies in NaCl films: strong electron-phonon coupling in double-barrier tunneling junctions. *Phys. Rev. Lett.* **95**, 225503 (2005).
35. Hebenstreit, W., Redinger, J., Horozova, Z., Schmid, M., Podloucky, R. and Varga, P., Atomic resolution by STM on ultra-thin films of alkali halides: experiment and local density calculations. *Surface Science* **424**, L321-L328 (1999).
36. Loppacher, C., Zerweck, U. and Eng, L.M., Kelvin probe force microscopy of alkali chloride thin films on Au (111). *Nanotechnology* **15**, S9 (2003).
37. Doniach, S., & Sunjic, M., Many-electron singularity in X-ray photoemission and X-ray line spectra from metals. *J. Physics C: Solid State Physics* **3**, 285 (1970).
38. Fuggle, J.C. and Mårtensson, N., Core-level binding energies in metals. *J. Electron Spectroscopy and Related Phenomena* **21**, 275 (1980)
39. Leiro, J., Minni, E., and Suoninen, E., Study of plasmon structure in XPS spectra of silver and gold. *J. Physics F: Metal Physics.* **13**, 215 (1983)
40. Espeter, P., Keutner, Ch., Roese, P., Shamout, K., Berges, U., and Westphal, C., Facing the interaction of absorbed silicon nano-ribbons on silver, *Nanotechnology* **28**, 455701 (2017)
41. Lagarde, P., Chorro, M., Roy, D., & Trcera, N. Study by EXAFS of the local structure around Si on silicene deposited on Ag (110) and Ag (111) surfaces. *J. Phys.: Cond. Mat.* **28**, 075002 (2016).
42. Lee, P.A., Teo, B.K. and Simons, A.L., EXAFS: A new parameterization of phase shifts. *J. Am. Chem. Soc.* **99**, 856-859 (1977).
43. Dujardin, G., Rose, F., Mayne, A. J., Toggling the local surface work function by pinning individual promoter atoms, *Phys. Rev. B* **63**, 235414 (2001).
44. Horcas, I., et al. WSXM: a software for scanning probe microscopy and a tool for nanotechnology. *Rev. Sci. Instrum*. **78**, 013705 (2007).
45. Ravel, B., & Newville, M. ATHENA, ARTEMIS, HEPHAESTUS: data analysis for X-ray absorption spectroscopy using IFEFFIT. *J. Synch. Rad.* **12**, 537-541 (2005).
46. Nilchian, M., Ward, J. P., Vonesch, C., & Unser, M. Optimized Kaiser–Bessel window functions for computed tomography. *IEEE Trans. Im. Process.* **24**, 3826-3833 (2015).
47. Lewis, J. P., Jelínek , P., Ortega, J., Demkov, A.A., Trabada, D. G., Haycock, B., Wang, H., Adams, G., Tomfoh, J. K., Abad, E., Wang H., Drabold D. A., Advances and applications in the FIREBALL ab initio tight-binding molecular-dynamics formalism. *Phys. Status Solidi B* **248**, 1989 (2011).
48. Basanta, M. A., Dappe, Y. J., Jelínek, P. and Ortega, Optimized atomic-like orbitals for first-principles tight-binding molecular dynamics. *J. Comput. Mater. Sci.* **39**, 759 (2007).
49. Sankey, O. F. and Niklewski, D. J., Ab initio multicenter tight-binding model for molecular-dynamics simulations and other applications in covalent systems. *Phys. Rev. B* **40**, 3979 (1989).
50. Silly, M. G., D'Angelo, M., Besson, M., Dappe, Y.J., Kubsky, S., Li, G., Nicolas, F., Pierucci, D., Thomasset, M., Electronic and structural properties of graphene-based metal-semiconducting heterostructures engineered by silicon intercalation. *Carbon* **76,** 27-39 (2014).

51. Dau, M. T., Gay, M., Di Felice, D., Vergnaud, C., Marty, A., Beigné, C., Renaud, G., Renault, O., Mallet, P., Le Quang, T., Veuillen, J.-Y., Huder, L., Renard, V. T., Chapelier, C., Zamborlini, G., Jugovac, M., Feyer, V., Dappe, Y. J., Pochet, P., and Jamet, M., Beyond van der Waals Interaction: The Case of MoSe2 Epitaxially Grown on Few-Layer Graphene. *ACS Nano* **12**, 2319-2331 (2018).